

CMR Scaling Law: Predicting Critical Mixture Ratios for Continual Pre-training of Language Models

Jiawei Gu^{§,†,1,2}, Zacc Yang^{†,2}, Chuanghao Ding^{2,3}, Rui Zhao², Fei Tan^{*,2}

¹Sun Yat-sen University

²SenseTime Research

³Nanjing University

¹kuvvius@gmail.com ²{yangzacc, zhaorui, tanfei}@sensetime.com ³ch777.ding@smail.nju.edu.cn

Abstract

Large Language Models (LLMs) excel in diverse tasks but often underperform in specialized fields due to limited domain-specific or proprietary corpus. Continual pre-training (CPT) enhances LLM capabilities by imbuing new domain-specific or proprietary knowledge while replaying general corpus to prevent catastrophic forgetting. The data mixture ratio of general corpus and domain-specific corpus, however, has been chosen heuristically, leading to sub-optimal training efficiency in practice. In this context, we attempt to re-visit the scaling behavior of LLMs under the hood of CPT, and discover a power-law relationship between loss, mixture ratio, and training tokens scale. We formalize the trade-off between general and domain-specific capabilities, leading to a well-defined Critical Mixture Ratio (CMR) of general and domain data. By striking the balance, CMR maintains the model’s general ability and achieves the desired domain transfer, ensuring the highest utilization of available resources. Considering the balance between efficiency and effectiveness, CMR can be regarded as the optimal mixture ratio. Through extensive experiments, we ascertain the predictability of CMR, propose CMR scaling law and have substantiated its generalization. These findings offer practical guidelines for optimizing LLM training in specialized domains, ensuring both general and domain-specific performance while efficiently managing training resources.

1 Introduction

Large Language Models (LLMs) exhibit versatile abilities, including question answering, translation, summarization, role-playing, etc. (Brown et al., 2020; Touvron et al., 2023a,b; Li et al., 2023; Lu et al., 2023). Their performance, however, may

degrade in specific domains due to limited corresponding pre-training data. To enhance LLMs’ abilities in specialized areas and avoid the enormous cost of re-training, a popular approach is Continual Pre-Training (CPT) (Colombo et al., 2024; Chen et al., 2023; Yıldız et al., 2024; Luo et al., 2023). This approaches are likely to equip LLMs with new domain-related capabilities without much general performance penalty.

Although CPT has been proven effective on multiple domains such as code (Li et al., 2023; Lei et al., 2024), law (Colombo et al., 2024) and medicine (Chen et al., 2023), the interplay among loss prediction and its scaling behavior with model size, and the number of training tokens is yet to be fully explored. Additionally, the composition of continual pre-training data is simply set up in a heuristic manner (Colombo et al., 2024; Chen et al., 2023), far from being principled. An inappropriate mixture ratio can lead to inefficient training (requiring excessive computation to adapt to specific domains) or insufficient training (failing to adequately reduce domain-specific loss). In light of this, three question hurdles we need to cross are as follows:

Does the optimal data mixture ratio exist for CPT? If so, how does it evolve with model scale or training token volume? Are there any involved simple yet principled laws?

Currently, several studies examine the scaling laws associated with different data mixture ratios. For instance, Ye et al. (2024) investigate how data mixtures shape scaling laws in the pre-training phase from the ground up, while Que et al. (2024) seek to pinpoint the optimal data mixture ratio in CPT, but overlook its crucial connection with the essential trade-off between general and domain loss in CPT.

Therefore, to strengthen our understanding about CPT and guide the experiments in the future, we attempt to address these questions with empirical

[§]Work was done during internship at SenseTime Research

[†]Equal contribution

^{*}Corresponding author

studies on CPT of LLMs. Specifically, we pre-train several LLMs with different model sizes from scratch and perform CPT on downstream domains (*Finance* and *Academic Papers*) with different data-mixture ratios. Our main contributions can be summarized as follows:

Formalization of the Trade-Off in CPT. We formalize the balance between domain-specific and general abilities during CPT by introducing the concept of feasible mixture ratios. CPT under feasible mixture ratios maintains performance on general data while enhancing performance on domain-specific data. We identify the maximum feasible mixture ratio as the **Critical Mixture Ratio (CMR)**, and regard it as the optimal mixture ratio by our definition.

Predictability of CMR. Through extensive experiments, we identify a power-law relationship between loss and both data-mixture ratio and training tokens. As such, we propose CMR scaling law to predict the best mixture ratio by scaling training token volume, which appears to be generalizable based on our findings.

Significance of CMR Scaling Law. CMR scaling law for CPT is crucial for efficient domain transfer for LLMs. This law allows us to determine the most efficient training configuration by predicting CMR using limited data and compute resources. The finding provides insights into the dynamics of CPT and may offer practical guidelines for optimizing LLM training in specialized domains.

2 Key Results

We train a series of LLMs with multiple mixture ratios of domain-specific data and general data to analyse the scaling behaviour in CPT. The method is detailed in § 3.2. Based on our experimental setup, we summarize the key results as follows:

1. The trade-off between two goals of CPT (Definition 1) suggests that, given a model of certain size, there exists a set of feasible mixture ratios (Definition 2) that achieve the goals under specific training data constraints.
2. Basically, general losses in CPT increase initially before decreasing, whereas domain losses tend to decrease. The relationships between loss and mixture ratio, as well as training volume, fit well with a power-law form, allowing for loss prediction under different mixture ratios and training tokens.

3. Using the loss prediction by mixture ratio and training volume, we can predict the CMR (Definition 3) with CMR scaling law.

- Given the maximum amount of training tokens, experiments in Figure 1 and predicted results in Figure 5 both show that CMR goes up with increasing model scale: from 29.8% for the 460M model to 34.9% for the 940M model.
- CMR depends on the similarity between the target domain and the general domain. The smaller the distribution gap between the two, the larger the CMR. Because *Academic Papers* constitute a larger portion of the general data than *Finance*, the pre-trained 460M model tends to show a higher CMR on *Academic Papers* (36.7%) compared to *Finance* (29.8%) during CPT, as illustrated in Figure 5 and Figure 6.

3 Background and Methods

The scaling law in the pre-training stage has been widely studied. In this work, we simplify the form of scaling law as much as possible, which is essentially consistent with previous works in § 6.

In this section, we will elaborate on the three main concepts involved in this work, including objective of CPT (Definition 1), feasible mixture ratio (Definition 2) and CMR (Definition 3). Then, we describe our experiment setups, including data preparation, experiment procedures and evaluation.

3.1 Continual Pre-training on Mixed Dataset

Definition 1. *Objective of CPT*

Given the pre-trained LLM M_S of model size S , general dataset \mathcal{D}_{gen} , and domain-specific dataset \mathcal{D}_{dom} , we continually pre-train M_S on a mixed dataset \mathcal{D}_R , where the **mixture ratio** of the domain-specific data is R , with $R \in [0, 1]$. The mixed dataset \mathcal{D}_R is denoted as $\mathcal{D}_R = \mathcal{D}_{\text{dom}} + \mathcal{D}_{\text{gen}}$ and $R = \frac{|\mathcal{D}_{\text{dom}}|}{(|\mathcal{D}_{\text{gen}}| + |\mathcal{D}_{\text{dom}}|)}$.

We define $\mathcal{L}_{\text{gen}/\text{dom}}(M_S)$ as the domain or general loss of the model M_S . We denote $\mathcal{L}_{\text{gen}/\text{dom}}^{\text{CPT}}(M_S, \mathcal{D}_R, T)$ as the domain/general loss of model M_S after CPT on dataset \mathcal{D}_R with training token volume T . Note that all losses mentioned above are validation losses. The goals for CPT are formalized as follows:

1. By the end of training, the general loss is supposed to either reach plateau or head downward

Domain-General Loss Curve

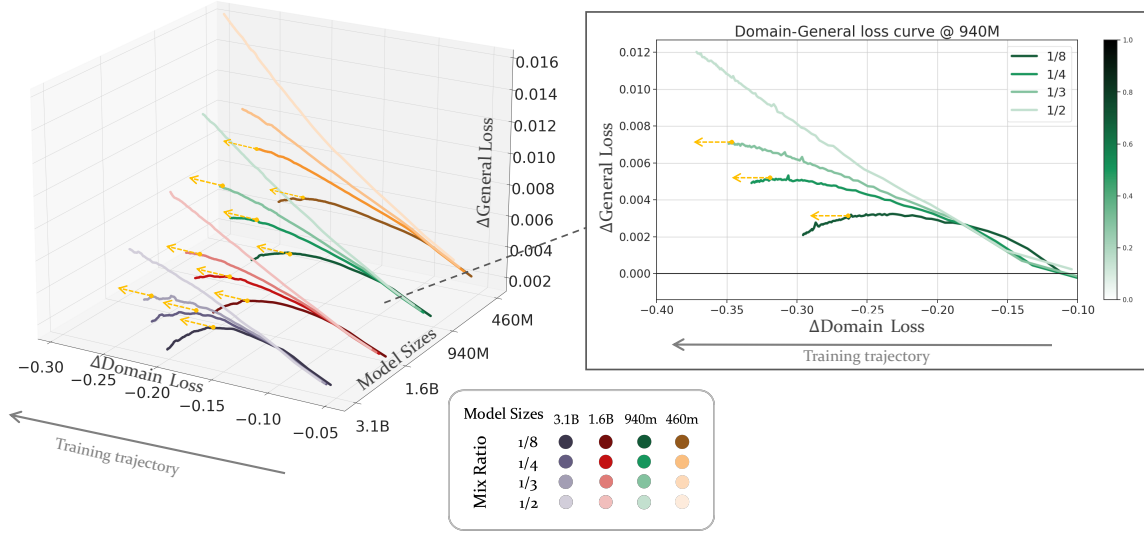


Figure 1: Follow the direction of the training trajectory to track the trend of the curve. Each bunch of lines represents a model size scale: $\{3.1\text{B}, 1.6\text{B}, 940\text{M}, 460\text{M}\}$ and each group of line colors represents the mixture ratios $\{1/8, 1/4, 1/3, 1/2\}$ from dark to light. In order to better display the trend, we have omitted proportions greater than $1/2$. The yellow dashed lines \leftarrow - point horizontally, indicating the corresponding ratios where $d\mathcal{L}_{\Delta\text{gen}}/d\mathcal{L}_{\Delta\text{dom}}$ closed to 0. The third set of lines of model size 940M, which has been zoomed in and depicted on the right side, showing the trend of the training curve more apparently. All horizontal and vertical cross-sections of the 3D diagram on the left side are detailed in the Appendix E.

(within a certain tolerance $\epsilon \geq 0$):

$$\mathcal{L}_{\text{gen}}^{\text{CPT}}(M_S, \mathcal{D}_R, T_{\max}) \leq \mathcal{L}_{\text{gen}}(M_S) + \epsilon. \quad (1)$$

2. Domain-specific loss should decline largely:

$$\mathcal{L}_{\text{dom}}^{\text{CPT}}(M_S, \mathcal{D}_R, T_{\max}) < \mathcal{L}_{\text{dom}}(M_S). \quad (2)$$

The increase in T from 0 to T_{\max} corresponds to the progression of the training trajectory. To better integrate these two aspects, we adopt the method of Lagrange multipliers (Rockafellar, 1993). The loss function $F(\cdot)$ for the whole objective of CPT is the Lagrangian as follows:

$$\begin{aligned} F(S, R, T, \lambda) = & \mathcal{L}_{\text{dom}}^{\text{CPT}}(M_S, \mathcal{D}_R, T) \\ & + \lambda(\mathcal{L}_{\text{gen}}^{\text{CPT}}(M_S, \mathcal{D}_R, T) \\ & - \mathcal{L}_{\text{gen}}(M_S) - \epsilon), \end{aligned} \quad (3)$$

where λ is the Lagrange multiplier used to enforce the constraint on the general loss while minimizing the domain-specific loss. In practice, λ governs the importance of two target dimensions in CPT. $F(S, R, T, \lambda)$ is the whole objective function.

Under resource constraints, the optimal training configuration should minimize \mathcal{L}_{dom} while satisfying the constraint on \mathcal{L}_{gen} , which involves finding

the optimal S , R , and T by solving the following optimization problem:

$$\begin{aligned} S^*, R^*, T^* = & \operatorname{argmin}_{M_S, R, T} F(S, R, T, \lambda), \\ \text{s.t.} \quad & \begin{cases} \mathcal{L}_{\text{gen}}^{\text{CPT}}(M_S, R, T_{\max}) \leq \mathcal{L}_{\text{gen}}(M_S) + \epsilon, \\ R \geq 0, T \geq 0, \lambda \geq 0. \end{cases} \end{aligned} \quad (4)$$

Definition 2. Feasible Mixture Ratio

Given fixed model size S , the optimization problem in Equation (3) can be boiled down to $F(R, T, \lambda)$. We first introduce a mixture ratio set \mathbb{A} : according to the first constraint of Definition 1, under a certain tolerance ϵ for the deterioration in the final general performance, we can choose a set of mixture ratios \mathbb{A} satisfying $\mathbb{A} = \{R \mid \mathcal{L}_{\text{gen}}^{\text{CPT}}(M_S, R, T_{\max}) \leq \mathcal{L}_{\text{gen}}(M_S) + \epsilon\}$. Ratios in \mathbb{A} that align with our CPT objective are considered as feasible mixture ratios, denoted as the set \mathbb{F} . A detailed definition transformation is presented in Appendix B.2, and here we directly provide the formula and the results of derivation: within the feasible mixture ratios, there exists a point T_0 over the training trajectory of CPT. As CPT proceeds with $T > T_0$, we have $\mathbb{F} = \{R \mid \exists T_0 \in (0, T_{\max}) : \frac{\partial F}{\partial T} \leq 0, R \in \mathbb{A}\}$.

An equivalent condition of defining \mathbb{F} can be

derived as:

$$\mathbb{F} = \{R \mid \exists T_0 \in [0, T_{\max}] : \left. \frac{\partial \mathcal{L}_{\Delta \text{gen}}(R, T)}{\partial \mathcal{L}_{\Delta \text{dom}}(R, T)} \right|_R = -\frac{1}{\lambda} < 0, R \in \mathbb{A}\}. \quad (5)$$

For simplicity, we have defined $\mathcal{L}_{\Delta \text{dom}} = \mathcal{L}_{\text{dom}}^{\text{CPT}} - \mathcal{L}_{\text{dom}}$ and $\mathcal{L}_{\Delta \text{gen}} = \mathcal{L}_{\text{gen}}^{\text{CPT}} - \mathcal{L}_{\text{gen}}$.

Visualization As shown in Figure 1, the training curves meeting the objective of CPT are marked with yellow dotted arrows, indicating the curves show a downward trend as training proceeds. The domain loss continuously decreases ($\mathcal{L}_{\Delta \text{dom}} \downarrow$) and the general loss is bounded ($d\mathcal{L}_{\Delta \text{gen}}/d\mathcal{L}_{\Delta \text{dom}} \rightarrow 0$) along the training trajectory until the ends of training. This visual representation effectively illustrates the behavior described by Equation (5), demonstrating the trade-off relationship between the domain loss and the general loss during training. The specific derivation and the interpretation of the slope for Figure 1 is detailed in Appendix B.2.

Definition 3. Critical Mixture Ratio (CMR)

Given limited compute resources and fixed model size, we hope that the language model can digest domain knowledge more efficiently by achieving the objective as described in Definition 1. Therefore, we define the maximum among feasible mixture ratios as the Critical Mixture Ratio (CMR) $R^* = \max\{R \mid R \in \mathbb{F}\}$.

The rationale is straightforward: if the ratio is less than CMR, the domain data is not sufficiently utilized in CPT; otherwise, the expected objective can't be achieved, which is manifested as an intolerable increase in general loss, leading to degradation in general ability. Thus, we argue that the CMR is the most suitable ratio for CPT due to the ideal balance of two sides.

3.2 Method

Data preparation Our general pre-training data is composed of corpora from Chinese, English, and code. The Chinese corpus and English corpus both include articles from encyclopedia, books, news, papers and social media sites. The code corpus is a subset sampled from StarCoder (Li et al., 2023). The general pre-training dataset comprises a total of 220 billion tokens. The proportions of Chinese, English, and code are roughly 44% : 36% : 20%.

We meticulously craft two specific domain datasets for CPT: *Finance* and *Academic Papers*.

The Finance dataset include financial news, financial policies and regulations, company announcements and research reports from securities and fund companies. The Academic Papers exclusively include papers from Arxiv. Each of the datasets contains at least 20 billion tokens, which is sufficient for our CPT.

Unless stated explicitly, all the following results are based on experiments with *Finance*. The results of CPT on *Academic Papers* are reported in § 5.3.

LLM Architecture The involved LLMs in this study have the same architecture as Llama series (Touvron et al., 2023a,b) with standard multi-head attention. The number of parameters ranges from 460M to 3.1B. The architecture is detailed in Table 1 of Appendix.

Experiment Setup We split the general pre-training dataset into two subsets: a 200B-token general dataset for general pre-training and a 20B-token general dataset for CPT.

In the pre-training stage, we pre-train the LLMs from scratch with 200B-token general dataset with a max learning rate of 3e-4, a batch size of 512, and a sequence length of 4096. The training step is 100,000 for each LLM. In the CPT stage, we train each LLM for another 10,000 steps (20 billion tokens) with a max learning rate of 3e-5 and warmup-constant LR schedule, on a mixture of the 20B-token general dataset and a domain dataset with different mixture ratios.

Evaluation Scaling laws emphasize the predictability of pre-training loss (Kaplan et al., 2020; Hoffmann et al., 2022; Gao et al., 2023; Hernandez et al., 2021), which is a widely-used performance indicator. Recent studies (Du et al., 2024; Yuan et al., 2023) highlight that pre-training loss is highly correlated with downstream task performance. Therefore, we use the pre-training loss on the validation set to measure the model's capability of general or domain-specific task during the CPT process. In addition, we use Mean Squared Error (MSE) and R-square (R^2) to measure the quality of the fitting, which provides a clear and interpretable analysis of the errors.

4 Does the Critical Mixture Ratio Exist?

— Yes, the CMR does exist.

A larger mixture ratio implies a higher proportion of domain-specific data in the training set, resulting

in a lower domain loss. However, due to the potential catastrophic forgetting of domain transfer, it is essential to ensure that the loss in the new domain continues to decrease while the original capabilities of LLMs are preserved and not compromised during CPT. Consequently, a higher mixture ratio is not always best. This raises an important question: does a Critical Mixture Ratio (CMR) exist that can balance these two goals of CPT in Definition 1 effectively and efficiently?

Figure 1 (left) demonstrates that for models of various sizes, there is at least one curve at a specific ratio that shows a downward trend, highlighted by yellow dotted arrows. This indicates the presence of feasible mixture ratios that align with our CPT objective. On the other hand, larger models tend to have bigger feasible mixture ratios set \mathbb{F} (more curves with yellow dotted arrows). For curves that meet the objective of CPT, a higher ratio is preferable, as it incorporates more domain knowledge while optimizing training efficiency within the tolerance of decline in general capacity. Therefore, the critical mixture ratio is defined as the highest proportion among these satisfactory curves, representing the optimal ratio for the given model size and limited training token volume.

If feasible ratios exist, we can conclude that CMR is also supposed to exist. Fundamentally, the existence of CMR arises from the trade-off between general and domain-specific capabilities, as well as the limited data and computing resources. According to definition 3, the CMR is present across models of different scales, as shown in Figure 1. This figure illustrates the existence of CMR as the maximum value within the feasible set. However, the precise value of CMR can not be determined from the figure, as it requires extensive experiments with different mixture ratios. The estimation of CMRs is discussed in 5.3 and plotted in Figure 5.

To look closely, we enlarged the longitudinal section of M_{940M} in the 3D graph in Figure 1 and placed it on the right side. It can be seen that as the mixture ratio increases, the curve continues to rise until the loss in the general domain exceeds our tolerance. The potentially controversial issue is that the downward trend in one-third of the curves is as clear as in the rest. The reason why it is feasible curve here can be found in Appendix B.2. Although it is not easily noticeable, there are indeed points on this curve where the slope is less than 0.

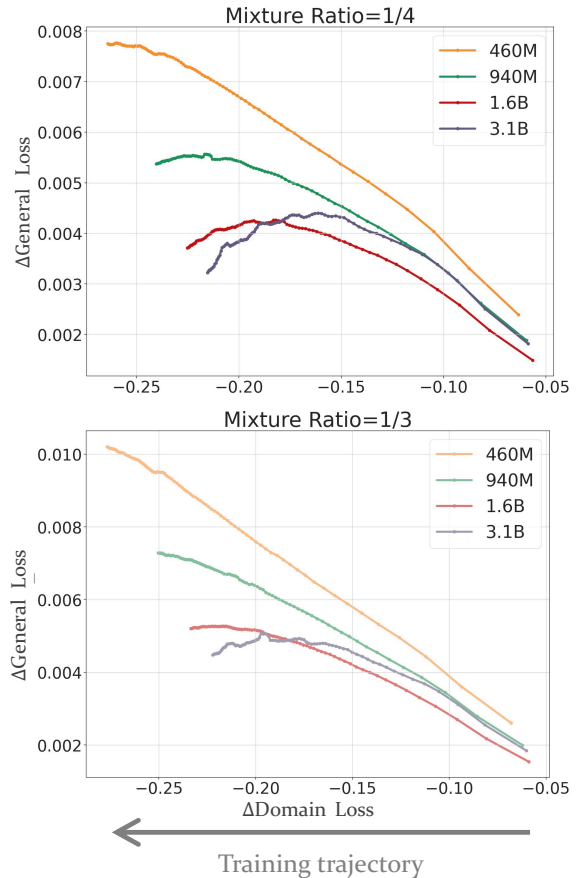


Figure 2: Follow the direction of the training trajectory to track the trend of the curve. The $\mathcal{L}_{\Delta_{\text{gen}}}$ and $\mathcal{L}_{\Delta_{\text{dom}}}$ loss functions for the models at mixture ratios of 1/4 and 1/3 are illustrated.

Findings From another perspective, we plot the loss curves of the models under the same mixture ratio as shown in Figure 2. When the mixture ratio is 1/4, all models can achieve the training objective of CPT. However, at a 1/3 mixture ratio, only M_{940M} , $M_{1.6B}$ and $M_{3.1B}$ achieve the CPT goal. This indicates that CMR for M_{940M} is around 1/4 within the scope of our training token volumes, while the CMRs for M_{940M} , $M_{1.6B}$ and $M_{3.1B}$ are at least 1/3. In other words, **CMRs slightly increase with model size, suggesting that larger models can accommodate a higher proportion of domain data.** We also further this finding by taking more cross-sections of Figure 1 (left) in Appendix E and the predicted CMR in following § 5.

This phenomenon can be explained by the models' ability to consume domain knowledge. As the proportion of domain-specific data increases, the knowledge that the model needs to learn also increases. LLMs with smaller size struggle to absorb much of domain knowledge while preserving the

general knowledge, leading to a degradation in their original general performance. In contrast, models with larger sizes can accommodate more knowledge with more parameters, thereby maintaining better performance.

5 Is CMR Predictable?

— Yes, the CMR can be predicted.

The existence of CMR indicates that in the process of CPT, we may explore the CMR scaling law to seek the best mixture ratio under resource constraints and domain data limitations, thereby optimizing training effectiveness and efficiency. In other words, the next question to answer is whether we can predict the CMR for model M_s given a maximum amount of continuation training token volume, T_{\max} .

To this end, two basic prerequisites must be met: predicting losses for different mixture ratio and predicting losses for different training token volume. In this section, we will demonstrate that these two prerequisites have been satisfied separately in § 5.1 and § 5.2, and finally detail the scaling law to predict CMR in § 5.3. To keep notations simple, we omit fixed variables in the loss function ($\mathcal{L}_{\text{dom/gen}}$ and $\mathcal{L}_{\Delta\text{dom}/\Delta\text{gen}}$) in this following.

5.1 Predicting Losses of Mixture Ratio

Predicting the general and domain loss is closely related to understanding the scaling behavior in the CPT stage. We study the scaling behavior of losses at $T = T_{\max}$. In addition, since scaling law aims to fit data points, their parametric forms should be intrinsically related to the observed trends in the data points. Based on previous works (Kaplan et al., 2020; Hoffmann et al., 2022) and data trends we observed, we proposed the simplified expression $\mathcal{L}(R)$ as a power-law form of

$$\mathcal{L}(R) = \alpha \cdot R^s + \beta,$$

where α is a coefficient, s is the exponent, and β is the bias.

As shown in Figure 3, domain loss gradually decreases with the increase of the mixture ratio, while general loss remains almost unchanged initially and then begins to rise. After fitting the general loss and domain loss separately for different mixture ratios R (non-endpoint values, $R \in (0, 1)$), we make predictions on new ratios. As shown in Figure 3, the predicted values align closely with the fitted curve. Notably, the predictions demonstrate

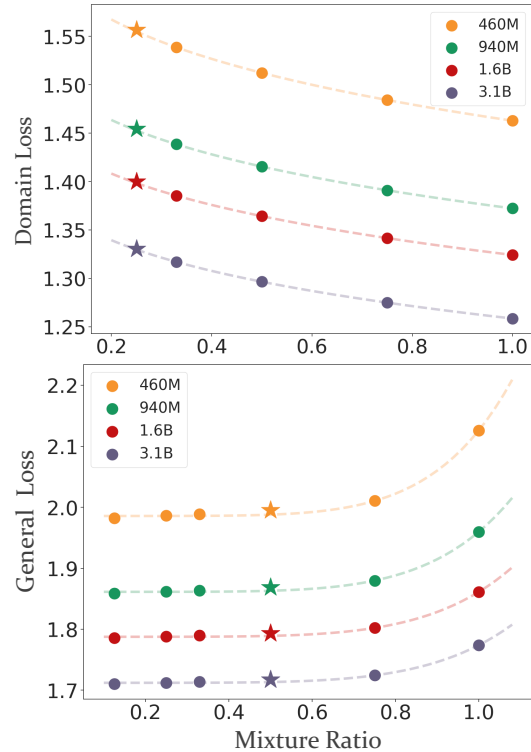


Figure 3: The upper figure shows the fitting curve of domain loss \mathcal{L}_{dom} with the change of mixture ratio R , and the lower figure shows the fitting curve of general loss \mathcal{L}_{gen} . The solid circles (●) represent real losses, and the stars (★) represent the predicted losses.

high accuracy, with error values within 0.05% as presented in Table 2.

Given the predicted $\mathcal{L}_{\text{dom}}(R)$ and $\mathcal{L}_{\text{gen}}(R)$ under different mixture ratios, we can obtain a range of mixture ratios that fulfil the tolerance limit ϵ , denoted as \mathbb{A} , according to Equation 3. In the objective of CPT we set, $\epsilon = 0.05$.

5.2 Predicting Losses of Training Tokens

Previous works (Kaplan et al., 2020; Hoffmann et al., 2022) have shown that the model size S and the volume of training tokens T can be used to fit the power law of loss. However, our work differs in two key aspects. First, we model the change of loss $\mathcal{L}_{\Delta\text{dom}/\Delta\text{gen}}(T)$ rather than the loss itself. Second, due to the phenomenon of general loss initially increasing and then decreasing as shown in Figure 4, we leverage a two-term polynomial function for better fitting. According to Equation 9 in Appendix B.2, the loss for CPT training tokens T is formulated as follows:

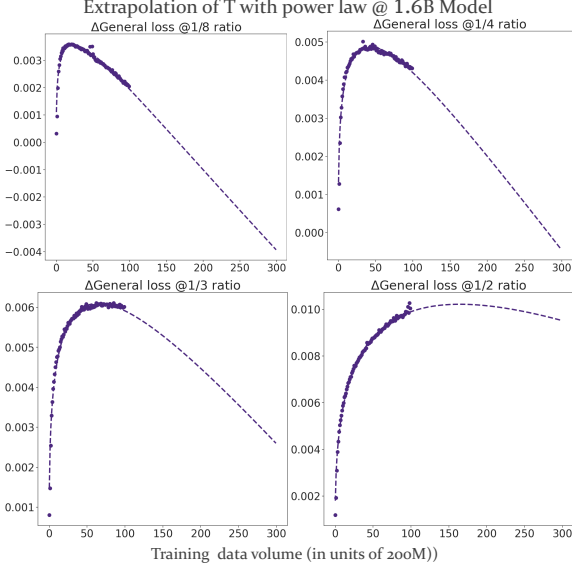


Figure 4: The figure shows the general loss of $M_{1.6B}$ fitting and extrapolating at four distinct mixture ratios: $\{1/8, 1/4, 1/3, 1/2\}$. As the ratio increases, the curve gradually rises when training data volume increases.

$$\begin{cases} \mathcal{L}_{\Delta\text{dom}}(T) = \alpha_1 \cdot T^{s_1} + \beta_1, \\ \mathcal{L}_{\Delta\text{gen}}(T) = \alpha_2 \cdot T^{s_2} + \alpha_3 \cdot T^{s_3} + \beta_2. \end{cases} \quad (6)$$

where $\alpha_1, \alpha_2, \alpha_3, \beta_1, \beta_2, s_1, s_2,$ and s_3 are learnable parameters. Our results demonstrate that the form (6) exhibits high fitting accuracy with low MSE and high R^2 in Table 3 and Figure 4.

5.3 Predicting CMR

According to the definition of feasible mixture ratios in Definition 2 and the method for determining the set \mathbb{F} in Appendix B.2, where $\mathbb{F} \subset \mathbb{A}$, and \mathbb{A} is obtained by predicting losses for any mixture ratio in § 5.1, we can establish a relationship between training token volume T and the feasible mixture ratios by the fitting laws in § 5.2. Overall, based on the parameters provided in Formula 6, the critical solution T_0 is obtained for a specific mixture ratio R_0 denoted as (derivation detailed in Appendix B.2):

$$T_0 = \left[-\frac{\alpha_1 \cdot s_1}{\lambda \alpha_2 \cdot s_2} \left(1 + \frac{\alpha_3 \cdot s_3}{\alpha_2 \cdot s_2} T_0^{s_3 - s_2} \right)^{-1} \right]^{\frac{1}{s_2 - s_1}} \quad (7)$$

When T_0 is less than the given maximum training token volume T_{\max} , we can conclude that the current ratio R_0 is a feasible mixture ratio. Conversely,

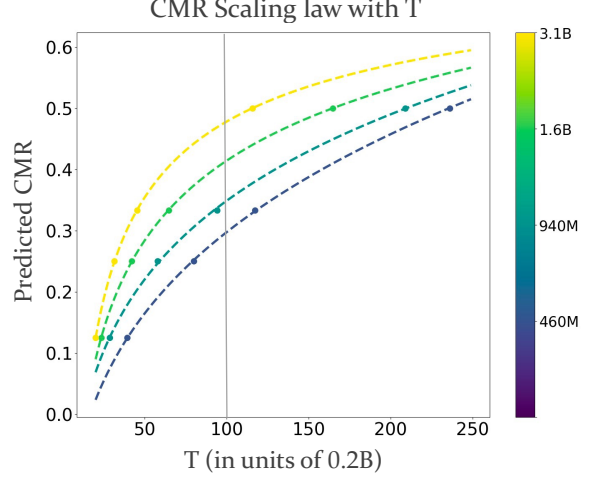


Figure 5: We can use the CMR scaling laws to predict CMRs under fixed model size S , and are extrapolated to $T = 250$, which is equivalent to a training volume of 500B tokens.

if T_0 exceeds T_{\max} , then R_0 is not a feasible mixture ratio. If T_0 is equal to T_{\max} , then R_0 is the critical ratio. We propose the following CMR scaling law:

$$R_{\text{CMR}} = \alpha_4 \cdot T^{s_4} + \beta_3. \quad (8)$$

The fitting curves are showed in Figure 5. In our experiments, T_{\max} is 20B tokens, which corresponds to a value of $T = 100$ in the figure. Therefore, for four models of different scales, their predicted CMR are 29.8%, 34.9%, 41.4% and 47.8% for $M_{460M}, M_{940M}, M_{1.6B}, M_{3.1B}$, respectively.

Generalization In order to verify whether the CMR scaling law can be generalized, we experiment on another domain *Academic Papers* with different mixture ratios. In this generalization experiment, we only conduct CPT on the 460M-sized model with *Academic Papers* data proportions set to $\{1/8, 1/4, 1/2, 3/4, 1/3\}$ respectively. All other settings were kept consistent with *Finance*. As shown in Figure 7, the trade-off of CPT still exist in this domain, and thus there exists a CMR. Furthermore, the CMR scaling law still work, which can observed in Figure 6. The predicted CMR for *Academic Papers* is 36.7%, given the maximum training token volume $T_{\max} = 100$.

Finding Comparing CMR predictions in two different domains, we find that the pre-trained model of the same size (460M) shows a higher CMR for *Academic Papers* (36.7%) compared to *Finance* (29.8%) during CPT. As illustrated in § 3.2, we

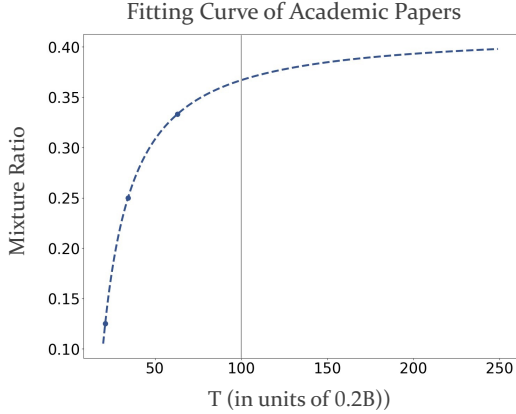


Figure 6: With a fixed model size $S = 460\text{M}$, using the CMR scaling law can be extrapolated to $T = 250$ and more. We can use the CMR scaling laws to predict CMR for *Academic Papers* in the CPT of $M_{460\text{M}}$. When $T = T_{\max} = 100$, the value of R is 36.7%, regarded as the CMR.

performed a statistical analysis on the general pre-training dataset, finding that data from the *Academic Papers* domain accounts for about 10%, while the *Finance* corpus is less than that. In other words, **the smaller the distribution gap between the target and general domains, the larger the CMR**. This observation aligns with related research findings (Ke et al., 2022, 2023) and can be attributed to the difficulty of domain adaptation. When the distribution gap between the target and general domains is smaller, domain adaptation becomes easier, reducing the risk of degradation of general performance during CPT, even with a higher proportion of domain-specific data.

Open Discussion As showed in Figs. 5 and 6, the larger the T_{\max} , the wider the range of feasible mixture ratios. Therefore, it seems that when T_{\max} tends to be infinity (the amount of data available for continued training is infinite, and computational resources are unlimited completely), the range of feasible mixture ratios would approach $(0, 1)$, leading CMR approaching 1. In this sense, each curve of CPT trajectory will show an expected convergence trend of objective, provided that there is enough T to allow it to develop.

Moreover, we find out that the solution of T_0 in Definition 2 approaches the inflexion point of $\mathcal{L}_{\Delta\text{gen}}(T)$ in Figure 4 and Figure 7, when $\lambda \rightarrow +\infty$, which we used for solving equations 14 ranges from 100 to 7000. The reason is likely to be that, the change in the general loss is much smaller

than the change in domain, and λ in the objective function of CPT needs to be very large to amplify such subtle changes within the tolerance of constraints. In addition, during the training process, the decreasing trend of domain loss has always been present, but there are obvious inflection points in the of general loss curve (rise first and then fall). That is to say, by only locating the inflection points on the general loss curve and finding this distance to the max training token volume, we can roughly estimate how far away we are from CMR at current ratio.

6 Related Work

6.1 Continual Pre-training

Continual Pre-Training (CPT) aims to perpetually pre-train large language models (LLMs), allowing them to adapt to new domains and reducing the high costs associated with training models from scratch for specialized tasks (Yıldız et al., 2024). CPT can be employed to tailor LLMs for specific fields, such as code (Lei et al., 2024; Li et al., 2023), medicine (Chen et al., 2023), law (Colombo et al., 2024), and science. By using an appropriate mixture of data from various domains (Gururangan et al., 2020), CPT not only enhances downstream performance but also mitigates the issue of catastrophic forgetting (Zhang et al., 2024), which is prevalent in all forms of post-training (Cossu et al., 2022; Luo et al., 2023).

Many recent studies on domain-specific LLMs (Chen et al., 2023; Colombo et al., 2024) adopt replay strategies (mixing general and domain-specific data) to concern about general losses during CPT. Other works (Que et al., 2024; Guo et al., 2024; Ge et al., 2024) have also noted challenges with maintaining general abilities, which aligns with our findings. For example, Guo et al. (2024) identified a *Stability Gap*, where performance initially drops during CPT and then gradually recovers, leading to inefficient pre-training and potential forgetting of general knowledge. In our work, we focus on the trade-off between general and domain-specific performance (losses) during CPT. To facilitate clearer experimental observations, we chose to restrict CPT to a single domain and did not explore the more complex setting of training across multiple domains.

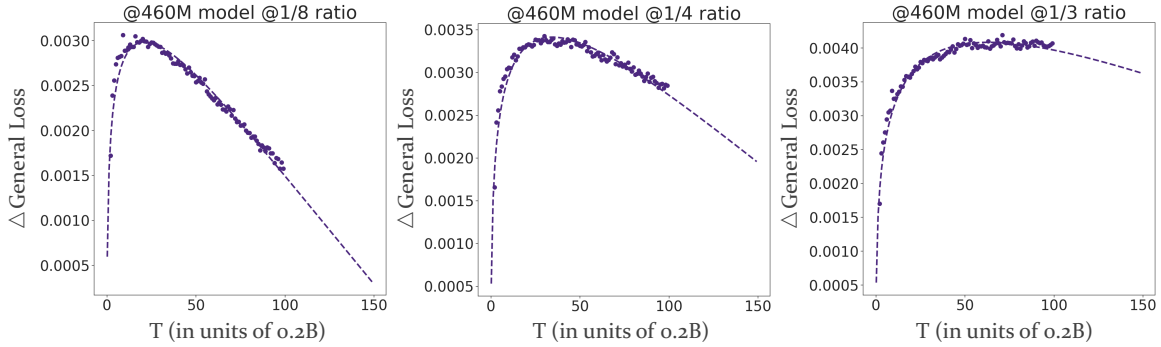


Figure 7: The figure shows the general loss of M_{460M} fitting and extrapolating at three distinct mixture ratios: $\{1/8, 1/4, 1/3\}$ with CPT on *Academic Papers*.

6.2 Scaling Law

Numerous studies (Hestness et al., 2017; Henighan et al., 2020; Bahri et al., 2021; Kaplan et al., 2020; Hoffmann et al., 2022; Yao and Wang, 2023) demonstrate a power-law relationship between performance and the increase in both the number of parameters and the size of the training data. These relationships are crucial for large language models (LLMs), being of paramount importance in various stages such as pre-training (Kaplan et al., 2020; Hoffmann et al., 2022; Ye et al., 2024), supervised fine-tuning (SFT) (Hernandez et al., 2021; Lin et al., 2024), etc. Recently, researchers describe scaling laws from various different perspectives (Pandey, 2024; Ye et al., 2024). The form of the scaling law used in this paper is consistent with Hoffmann et al. (2022), $L = E + \frac{A}{S^\alpha} + \frac{B}{T^\beta}$, where $\{E, A, B, \alpha, \beta\}$ are fitting parameters. However, we express in a simpler and more appropriate way for our demonstrations.

6.3 Data Mixture Scaling Law

Several studies have examined the scaling laws associated with various data mixture ratios. For instance, Ye et al. (2024) investigate how different data mixtures influence scaling laws during the pre-training phase. However, their proposed laws are not applicable to CPT. Another study by Que et al. (2024) aims to identify the optimal data mixture ratio using the D-CPT law. Their method focuses solely on minimizing domain loss by fixing model sizes and training token volume, thereby neglecting the trade-off between general loss and domain loss, which is critical in CPT.

7 Conclusion

In this work, we investigated the scaling behavior of LLMs under Continual Pre-Training (CPT) to

address the limitations of domain-specific performance. We provided a clear definition of Critical Mixture Ratio (CMR) for optimizing the mixture ratio of general and domain-specific data. Our experiments revealed a power-law relationship between loss, mixture ratio, and training data size, allowing us to predict the CMR efficiently. These findings may offer practical guidelines for optimizing LLM training, helping to balance general and domain-specific performance while minimizing resource consumption. Additionally, our study suggests that understanding the CPT process and scaling laws could be valuable for future research aimed at enhancing LLM capabilities in specialized fields.

8 Limitations

Computational Constraints We experimented with model sizes range from 400M to 3.1B. However, the largest model in our experiments is still relatively small among contemporary LLMs. It may lead to inaccuracy in estimation of model size scaling.

Limited Domains In this work, we conducted continual pre-training only on two specific domains (finance and academic papers) respectively. Although we have drawn some useful conclusions from the experimental results, experiments with more domains are expected to provide more refined results and likely to bring some new insights.

CMR scaling law with model size The CMR scaling in this work can only predict the CMR of a fixed model size. We have not explored how to predict CMR of large models with experiments on small models. A possible method is that first we extrapolate all the losses of small models to large models with model size scaling law, and use CMR

scaling law to predict the CMR of the large model. We left it as a future work to predict CMR by leveraging multiple scaling laws with less computational efforts.

Downstream Evaluation As stated in § 3.2, our primary focus was on establishing and validating the CMR scaling law through loss metrics, which is widely used and highly correlated with downstream task performance. However, this study did not directly evaluate performance on downstream tasks. Including downstream task performance could provide a more intuitive understanding of the observed trends.

References

- Yasaman Bahri, Ethan Dyer, Jared Kaplan, Jaehoon Lee, and Utkarsh Sharma. 2021. Explaining neural scaling laws. *arXiv preprint arXiv:2102.06701*.
- Tom B. Brown, Benjamin Mann, Nick Ryder, Melanie Subbiah, Jared Kaplan, Prafulla Dhariwal, Arvind Neelakantan, Pranav Shyam, Girish Sastry, Amanda Askell, Sandhini Agarwal, Ariel Herbert-Voss, Gretchen Krueger, Tom Henighan, Rewon Child, Aditya Ramesh, Daniel M. Ziegler, Jeffrey Wu, Clemens Winter, Christopher Hesse, Mark Chen, Eric Sigler, Mateusz Litwin, Scott Gray, Benjamin Chess, Jack Clark, Christopher Berner, Sam McCandlish, Alec Radford, Ilya Sutskever, and Dario Amodei. 2020. [Language models are few-shot learners](#). *Preprint*, arXiv:2005.14165.
- Zeming Chen, Alejandro Hernández Cano, Angelika Romanou, Antoine Bonnet, Kyle Matoba, Francesco Salvi, Matteo Pagliardini, Simin Fan, Andreas Köpf, Amirkeivan Mohtashami, et al. 2023. Meditron-70b: Scaling medical pretraining for large language models. *arXiv preprint arXiv:2311.16079*.
- Pierre Colombo, Telmo Pessoa Pires, Malik Boudiaf, Dominic Culver, Rui Melo, Caio Corro, Andre FT Martins, Fabrizio Esposito, Vera Lúcia Raposo, Sofia Morgado, et al. 2024. Saullm-7b: A pioneering large language model for law. *arXiv preprint arXiv:2403.03883*.
- Andrea Cossu, Tinne Tuytelaars, Antonio Carta, Lucia Passaro, Vincenzo Lomonaco, and Davide Bacciu. 2022. Continual pre-training mitigates forgetting in language and vision. *arXiv preprint arXiv:2205.09357*.
- Zhengxiao Du, Aohan Zeng, Yuxiao Dong, and Jie Tang. 2024. Understanding emergent abilities of language models from the loss perspective. *arXiv preprint arXiv:2403.15796*.
- Leo Gao, John Schulman, and Jacob Hilton. 2023. Scaling laws for reward model overoptimization. In *International Conference on Machine Learning*, pages 10835–10866. PMLR.
- Ce Ge, Zhijian Ma, Daoyuan Chen, Yaliang Li, and Bolin Ding. 2024. Data mixing made efficient: A bivariate scaling law for language model pretraining. *arXiv preprint arXiv:2405.14908*.
- Yiduo Guo, Jie Fu, Huishuai Zhang, Dongyan Zhao, and Yikang Shen. 2024. Efficient continual pre-training by mitigating the stability gap. *arXiv preprint arXiv:2406.14833*.
- Suchin Gururangan, Ana Marasović, Swabha Swayamdipta, Kyle Lo, Iz Beltagy, Doug Downey, and Noah A. Smith. 2020. [Don’t stop pretraining: Adapt language models to domains and tasks](#). In *Proceedings of the 58th Annual Meeting of the Association for Computational Linguistics*, pages 8342–8360, Online. Association for Computational Linguistics.
- Tom Henighan, Jared Kaplan, Mor Katz, Mark Chen, Christopher Hesse, Jacob Jackson, Heewoo Jun, Tom B Brown, Prafulla Dhariwal, Scott Gray, et al. 2020. Scaling laws for autoregressive generative modeling. *arXiv preprint arXiv:2010.14701*.
- Danny Hernandez, Jared Kaplan, Tom Henighan, and Sam McCandlish. 2021. Scaling laws for transfer. *arXiv preprint arXiv:2102.01293*.
- Joel Hestness, Sharan Narang, Newsha Ardalani, Gregory Diamos, Heewoo Jun, Hassan Kianinejad, Md Mostofa Ali Patwary, Yang Yang, and Yanqi Zhou. 2017. Deep learning scaling is predictable, empirically. *arXiv preprint arXiv:1712.00409*.
- Jordan Hoffmann, Sebastian Borgeaud, Arthur Mensch, Elena Buchatskaya, Trevor Cai, Eliza Rutherford, Diego de Las Casas, Lisa Anne Hendricks, Johannes Welbl, Aidan Clark, et al. 2022. Training compute-optimal large language models. *arXiv preprint arXiv:2203.15556*.
- Jared Kaplan, Sam McCandlish, Tom Henighan, Tom B Brown, Benjamin Chess, Rewon Child, Scott Gray, Alec Radford, Jeffrey Wu, and Dario Amodei. 2020. Scaling laws for neural language models. *arXiv preprint arXiv:2001.08361*.
- Zixuan Ke, Haowei Lin, Yijia Shao, Hu Xu, Lei Shu, and Bing Liu. 2022. Continual training of language models for few-shot learning. *arXiv preprint arXiv:2210.05549*.
- Zixuan Ke, Yijia Shao, Haowei Lin, Tatsuya Konishi, Gyuhak Kim, and Bing Liu. 2023. Continual pre-training of language models. *arXiv preprint arXiv:2302.03241*.
- Bin Lei, Yuchen Li, and Qiuwu Chen. 2024. Autocoder: Enhancing code large language model with \textsc{AIEV-Instruct}. *arXiv preprint arXiv:2405.14906*.
- Raymond Li, Loubna Ben Allal, Yangtian Zi, Niklas Muennighoff, Denis Kocetkov, Chenghao Mou, Marc Marone, Christopher Akiki, Jia Li, Jenny Chim, Qian Liu, Evgenii Zheltonozhskii, Terry Yue Zhuo,

- Thomas Wang, Olivier Dehaene, Mishig Davaadorj, Joel Lamy-Poirier, João Monteiro, Oleh Shliazhko, Nicolas Gontier, Nicholas Meade, Armel Zebaze, Ming-Ho Yee, Logesh Kumar Umapathi, Jian Zhu, Benjamin Lipkin, Muhtasham Oblokulov, Zhiruo Wang, Rudra Murthy, Jason Stillerman, Siva Sankalp Patel, Dmitry Abulkhanov, Marco Zocca, Manan Dey, Zhihan Zhang, Nour Fahmy, Urvashi Bhattacharyya, Wenhao Yu, Swayam Singh, Sasha Luccioni, Paulo Villegas, Maxim Kunakov, Fedor Zhdanov, Manuel Romero, Tony Lee, Nadav Timor, Jennifer Ding, Claire Schlesinger, Hailey Schoelkopf, Jan Ebert, Tri Dao, Mayank Mishra, Alex Gu, Jennifer Robinson, Carolyn Jane Anderson, Brendan Dolan-Gavitt, Danish Contractor, Siva Reddy, Daniel Fried, Dzmitry Bahdanau, Yacine Jernite, Carlos Muñoz Ferrandis, Sean Hughes, Thomas Wolf, Arjun Guha, Leandro von Werra, and Harm de Vries. 2023. [Starcoder: may the source be with you!](#) *Preprint*, arXiv:2305.06161.
- Haowei Lin, Baizhou Huang, Haotian Ye, Qinyu Chen, Zihao Wang, Sujian Li, Jianzhu Ma, Xiaojun Wan, James Zou, and Yitao Liang. 2024. Selecting large language model to fine-tune via rectified scaling law. *arXiv preprint arXiv:2402.02314*.
- Jinghui Lu, Dongsheng Zhu, Weidong Han, Rui Zhao, Brian Mac Namee, and Fei Tan. 2023. What makes pre-trained language models better zero-shot learners? In *Proceedings of the 61st Annual Meeting of the Association for Computational Linguistics (Volume 1: Long Papers)*, pages 2288–2303.
- Yun Luo, Zhen Yang, Fandong Meng, Yafu Li, Jie Zhou, and Yue Zhang. 2023. An empirical study of catastrophic forgetting in large language models during continual fine-tuning. *arXiv preprint arXiv:2308.08747*.
- Rohan Pandey. 2024. gzip predicts data-dependent scaling laws. *arXiv preprint arXiv:2405.16684*.
- Haoran Que, Jiaheng Liu, Ge Zhang, Chenchen Zhang, Xingwei Qu, Yinghao Ma, Feiyu Duan, Zhiqi Bai, Jiakai Wang, Yuanxing Zhang, et al. 2024. D-cpt law: Domain-specific continual pre-training scaling law for large language models. *arXiv preprint arXiv:2406.01375*.
- R Tyrrell Rockafellar. 1993. Lagrange multipliers and optimality. *SIAM review*, 35(2):183–238.
- Hugo Touvron, Thibaut Lavril, Gautier Izacard, Xavier Martinet, Marie-Anne Lachaux, Timothée Lacroix, Baptiste Rozière, Naman Goyal, Eric Hambro, Faisal Azhar, Aurelien Rodriguez, Armand Joulin, Edouard Grave, and Guillaume Lample. 2023a. [Llama: Open and efficient foundation language models](#). *Preprint*, arXiv:2302.13971.
- Hugo Touvron, Louis Martin, Kevin Stone, Peter Albert, Amjad Almahairi, Yasmine Babaei, Nikolay Bashlykov, Soumya Batra, Prajjwal Bhargava, Shrutu Bhosale, Dan Bikel, Lukas Blecher, Cristian Canton Ferrer, Moya Chen, Guillem Cucurull, David Esiobu, Jude Fernandes, Jeremy Fu, Wenyin Fu, Brian Fuller, Cynthia Gao, Vedanuj Goswami, Naman Goyal, Anthony Hartshorn, Saghar Hosseini, Rui Hou, Hakan Inan, Marcin Kardas, Viktor Kerkez, Madian Khabsa, Isabel Kloumann, Artem Korenev, Punit Singh Koura, Marie-Anne Lachaux, Thibaut Lavril, Jenya Lee, Diana Liskovich, Yinghai Lu, Yuning Mao, Xavier Martinet, Todor Mihaylov, Pushkar Mishra, Igor Molybog, Yixin Nie, Andrew Poulton, Jeremy Reizenstein, Rashi Rungta, Kalyan Saladi, Alan Schelten, Ruan Silva, Eric Michael Smith, Ranjan Subramanian, Xiaoqing Ellen Tan, Binh Tang, Ross Taylor, Adina Williams, Jian Xiang Kuan, Puxin Xu, Zheng Yan, Iliyan Zarov, Yuchen Zhang, Angela Fan, Melanie Kambadur, Sharan Narang, Aurelien Rodriguez, Robert Stojnic, Sergey Edunov, and Thomas Scialom. 2023b. [Llama 2: Open foundation and fine-tuned chat models](#). *Preprint*, arXiv:2307.09288.
- Yiqun Yao and Yequan Wang. 2023. Research without re-search: Maximal update parametrization yields accurate loss prediction across scales. *arXiv preprint arXiv:2304.06875*.
- Jiasheng Ye, Peiju Liu, Tianxiang Sun, Yunhua Zhou, Jun Zhan, and Xipeng Qiu. 2024. Data mixing laws: Optimizing data mixtures by predicting language modeling performance. *arXiv preprint arXiv:2403.16952*.
- Çağatay Yıldız, Nishaanth Kanna Ravichandran, Prishruit Punia, Matthias Bethge, and Beyza Ermis. 2024. Investigating continual pretraining in large language models: Insights and implications. *arXiv preprint arXiv:2402.17400*.
- Zheng Yuan, Hongyi Yuan, Chengpeng Li, Guanting Dong, Chuanqi Tan, and Chang Zhou. 2023. Scaling relationship on learning mathematical reasoning with large language models. *arXiv preprint arXiv:2308.01825*.
- Hengyuan Zhang, Yanru Wu, Dawei Li, Zacc Yang, Rui Zhao, Yong Jiang, and Fei Tan. 2024. Balancing speciality and versatility: a coarse to fine framework for supervised fine-tuning large language model. *arXiv preprint arXiv:2404.10306*.

A LLM Configurations

The detailed parameters of the LLM configurations are listed in Table 1.

Table 1: Configurations of the LLMs.

Model Size	460m	940M	1.6B	3.1B
hidden size	1024	1536	2048	2560
intermediate size	3072	4608	6144	7680
number of attention heads	32	32	32	32
number of layers	24	24	24	32
vocabulary size	65632	65632	65632	65632

B Mathematical derivation

B.1 Notation

- S - represents the model sizes.
- M - the pre-trained large language model.
- \mathcal{D}_{gen} - the general dataset.
- \mathcal{D}_{dom} - the domain-specific dataset.
- R - the mixture ratio of the domain-specific data.
- \mathcal{D}_R - the total mixed dataset with $R\%$ domain-specific data.
- ϵ - tolerance for the general loss increase.
- $\mathcal{L}_{\text{gen}}^{\text{CPT}}$ - the general loss.
- $\mathcal{L}_{\text{dom}}^{\text{CPT}}$ - the domain-specific loss.
- $\mathcal{L}_{\Delta\text{gen}}$ - the increment in general loss.
- $\mathcal{L}_{\Delta\text{dom}}$ - the increment in domain-specific loss.
- F - the loss function of CPT expressed as the Lagrangian.
- T - the amount of training tokens (related to the number of iterations, training steps, or the total volume of training data).
- λ - the Lagrange multiplier used to enforce the constraint on general loss while minimizing domain-specific loss.
- T_{max} - the maximum training tokens for CPT.
- T_0 - a point on the training curve where, after training at T_0 and continuing the training, the feasible mixture ratio is observed.
- \mathbb{A} - the set of mixture ratios that satisfying CPT objective.
- \mathbb{F} - the set of Feasible Mixture Ratios (feasible mixture ratio).
- R_{CMR} - the Critical Mixture Ratio (CMR), which is the optimal mixture ratio that minimizes the loss function within the feasible set.

- $\alpha_1, \alpha_2, \alpha_3$ - parameters to be fitted representing coefficients in the power-law functions for the increment of loss.
- β_1, β_2 - parameters to be fitted representing constants in the power-law functions for the increment of loss.
- s_1, s_2, s_3 - parameters to be fitted representing the exponents in the power-law functions for the increment of loss.

B.2 Feasible mixture ratio

Given that N is fixed, the Objective of CPT in Equation 3 can be transformed into:

$$F(R, T, \lambda) = (\mathcal{L}_{\text{dom}}(M_S) + \mathcal{L}_{\Delta\text{dom}}(R, T)) + \lambda(\mathcal{L}_{\Delta\text{gen}}(\mathcal{R}, T) - \epsilon), \quad (9)$$

where $\mathcal{L}_{\text{dom}}(\text{CPT}(M_S; \mathcal{D}_R, T))$ is split into the value at $T = 0$, $\mathcal{L}_{\text{dom}}(M_S)$ and the increment $\mathcal{L}_{\Delta\text{dom}}$. The corresponding

$$R^* = \underset{R}{\text{argmin}} F(R, T, \lambda) \quad \text{s.t.} \quad \begin{cases} \mathcal{L}_{\Delta\text{gen}}(R, T) \leq \epsilon \\ R \geq 0 \\ T_{\text{max}} \geq T \geq 0 \\ \lambda \geq 0. \end{cases} \quad (10)$$

For a given mixture ratio R , if the training progresses (T increases), and the objective function (Equation 9) shows a decreasing trend, it indicates that the current proportion can lead to the continuation of training towards the expected goal. The trend of the objective function F increasing with training can be reflected by its partial derivative with respect to T :

$$\left. \frac{\partial F(R, T, \lambda)}{\partial T} \right|_{R, \lambda} = \left. \frac{\partial (\mathcal{L}_{\text{dom}}(M_S) + \mathcal{L}_{\Delta\text{dom}}(R, T))}{\partial T} \right|_{R, \lambda} + \lambda \left. \frac{\partial (\mathcal{L}_{\Delta\text{gen}}(R, T) - \epsilon)}{\partial T} \right|_{R, \lambda}. \quad (11)$$

Since $\mathcal{L}_{\text{dom}}(M_S)$ and $-\lambda\epsilon$ are constants with respect to T , their derivatives are zero. Thus, we simplify to:

$$\left. \frac{\partial F(R, T, \lambda)}{\partial T} \right|_{R, \lambda} = \left. \frac{\partial \mathcal{L}_{\Delta\text{dom}}(R, T)}{\partial T} \right|_{R, \lambda} + \lambda \left. \frac{\partial \mathcal{L}_{\Delta\text{gen}}(R, T)}{\partial T} \right|_{R, \lambda}. \quad (12)$$

If the training objective under the fixed ratio progresses as expected, there should be at least one point during the training process ($0 \leq T \leq T_{\text{max}}$) where this partial derivative is less than or equal to 0. From this, we can define a feasible proportion curve that should satisfy the following inequality conditions:

$$\exists T \in [0, T_{\text{max}}] : \left. \frac{\partial F(R, T, \lambda)}{\partial T} \right|_{R, \lambda} \leq 0 \quad (13)$$

This means that we only need to determine whether the solution T of the above inequality 13 belongs to $[0, T_{\text{max}}]$ in order to judge whether the current training meets the target. Setting it equal to zero to figure out:

$$\left. \frac{\partial F(R, T, \lambda)}{\partial T} \right|_{R, \lambda} = 0 \quad (14)$$

Setting the equation to zero and further simplifying to express it:

$$\left. \frac{\partial \mathcal{L}_{\Delta\text{dom}}(R, T)}{\partial T} \right|_R + \lambda \left. \frac{\partial \mathcal{L}_{\Delta\text{gen}}(R, T)}{\partial T} \right|_R = 0 \quad (15)$$

To derive the following equation using the chain rule:

$$\left. \frac{\partial \mathcal{L}_{\Delta\text{dom}}(R, T)}{\partial T} \right|_R = -\lambda \left. \frac{\partial \mathcal{L}_{\Delta\text{gen}}(R, T)}{\partial T} \right|_R \quad (16)$$

By isolating $\left. \frac{\partial \mathcal{L}_{\Delta \text{dom}}(R, T)}{\partial T} \right|_R$, we get:

$$\left. \frac{\partial \mathcal{L}_{\Delta \text{dom}}(R, T)}{\partial T} \right|_R = -\lambda \left. \frac{\partial \mathcal{L}_{\Delta \text{gen}}(R, T)}{\partial T} \right|_R \quad (17)$$

Using the chain rule, we have:

$$\left. \frac{\partial \mathcal{L}_{\Delta \text{gen}}(R, T)}{\partial T} \right|_R = \left. \frac{\partial \mathcal{L}_{\Delta \text{gen}}(R, T)}{\partial \mathcal{L}_{\Delta \text{dom}}(R, T)} \right|_R \cdot \left. \frac{\partial \mathcal{L}_{\Delta \text{dom}}(R, T)}{\partial T} \right|_R \quad (18)$$

By substituting this into the given equation, we get:

$$\left. \frac{\partial \mathcal{L}_{\Delta \text{dom}}(R, T)}{\partial T} \right|_R = -\lambda \left(\left. \frac{\partial \mathcal{L}_{\Delta \text{gen}}(R, T)}{\partial \mathcal{L}_{\Delta \text{dom}}(R, T)} \right|_R \cdot \left. \frac{\partial \mathcal{L}_{\Delta \text{dom}}(R, T)}{\partial T} \right|_R \right) \quad (19)$$

Assuming $\left. \frac{\partial \mathcal{L}_{\Delta \text{dom}}(R, T)}{\partial T} \right|_R \neq 0$, we can cancel the terms:

$$1 = -\lambda \cdot \left. \frac{\partial \mathcal{L}_{\Delta \text{gen}}(R, T)}{\partial \mathcal{L}_{\Delta \text{dom}}(R, T)} \right|_R \quad (20)$$

Thus, we obtain:

$$\left. \frac{\partial \mathcal{L}_{\Delta \text{gen}}(R, T)}{\partial \mathcal{L}_{\Delta \text{dom}}(R, T)} \right|_R = -\frac{1}{\lambda} \quad (21)$$

Since $\lambda > 0$, the above derivative is a negative number. For a specific R , if there exist points on the training curve where the partial derivatives of the two Δ values are equal to $\frac{1}{\lambda}$, then the ratio is consistent with the expected goal of continual pretraining. These ratios are called feasible mixture ratios, and their set is denoted as \mathbb{F} . This is consistent with the feasible mixture ratios marked in Figure 1.

B.3 Fitting

Following the previous work (Kaplan et al., 2020; Hoffmann et al., 2022), we have adopted the power-law as the parametric forms, which is different from other mixture law study (Ye et al., 2024). Previous work has shown that the model parameter N and the amount of data training T are independently related to the power law of loss. However, one point that our work related to power law is different. First, the function we choose to fit is the increment of Loss. Second, due to the phenomenon of general loss increasing first and then decreasing, in order to better fit the data, we used a two-term power-law function. According to Equation 9, the data mixture scaling law for CPT training is defined as follows:

Given:

$$\begin{cases} \mathcal{L}_{\Delta \text{dom}}(T) = \alpha_1 \cdot T^{s1} + \beta_1, \\ \mathcal{L}_{\Delta \text{gen}}(T) = \alpha_2 \cdot T^{s2} + \alpha_3 \cdot T^{s3} + \beta_2. \end{cases} \quad (22)$$

where $\alpha_1, \alpha_2, \alpha_3, \beta_1, \beta_2, s1, s2$, and $s3$ are parameters to be fitted.

First, according to the definition of feasible mixture ratios, we can solve feasible mixture ratios under the setting of data mixture scaling law. As the fitting at this time is an extrapolation of the training quantity, R is a fixed value. For simplicity, we no longer explicitly write R , so both $\mathcal{L}_{\Delta \text{dom}}$ and $\mathcal{L}_{\Delta \text{gen}}$ are univariate functions of T . First, differentiate $\mathcal{L}_{\Delta \text{dom}}(T)$ with respect to T :

$$\begin{aligned} \frac{d}{dT} \mathcal{L}_{\Delta \text{dom}}(T) &= \frac{d}{dT} (\alpha_1 \cdot T^{s1} + \beta_1) \\ &= \alpha_1 \cdot s1 \cdot T^{s1-1}. \end{aligned} \quad (23)$$

Next, differentiate $\mathcal{L}_{\Delta \text{gen}}(T)$ with respect to T :

$$\frac{d}{dT} \mathcal{L}_{\Delta \text{gen}}(T) = \frac{d}{dT} (\alpha_2 \cdot T^{s2} + \alpha_3 \cdot T^{s3} + \beta_2) = \alpha_2 \cdot s2 \cdot T^{s2-1} + \alpha_3 \cdot s3 \cdot T^{s3-1}. \quad (24)$$

According to the the expected CPT trend in Equation 13, we need to figure whether the critical T_0 that meets this condition is in the effective range $[0, T_{\max}]$. Therefore, the solution for the Equation 15 is important, which can be solved as Equation 15:

$$\frac{d}{dT}\mathcal{L}_{\Delta\text{dom}}(T) + \lambda\frac{d}{dT}\mathcal{L}_{\Delta\text{gen}}(T) = 0 \quad (25)$$

Substitute Equation 23 and Equation 24 respectively, we get:

$$\alpha_1 \cdot s_1 \cdot T^{s_1-1} + \lambda(\alpha_2 \cdot s_2 \cdot T^{s_2-1} + \alpha_3 \cdot s_3 \cdot T^{s_3-1}) = 0 \quad (26)$$

Further simplifying:

$$\alpha_1 \cdot s_1 \cdot T^{s_1-1} + \lambda\alpha_2 \cdot s_2 \cdot T^{s_2-1} + \lambda\alpha_3 \cdot s_3 \cdot T^{s_3-1} = 0 \quad (27)$$

To solve for T , we can factor out T terms:

$$T^{s_1-1}(\alpha_1 \cdot s_1 + \lambda\alpha_2 \cdot s_2 \cdot T^{s_2-s_1} + \lambda\alpha_3 \cdot s_3 \cdot T^{s_3-s_1}) = 0 \quad (28)$$

Therefore, the critical points T_0 can be solved by:

$$T_0^{s_2-s_1} = -\frac{\alpha_1 \cdot s_1}{\lambda\alpha_2 \cdot s_2} - \frac{\lambda\alpha_3 \cdot s_3 \cdot T_0^{s_3-s_1}}{\lambda\alpha_2 \cdot s_2} \quad (29)$$

Solving for T_0 :

$$T_0^{s_2-s_1} = -\frac{\alpha_1 \cdot s_1 + \lambda\alpha_3 \cdot s_3 \cdot T_0^{s_3-s_1}}{\lambda\alpha_2 \cdot s_2} \quad (30)$$

$$T_0^{s_2-s_1} = -\frac{\alpha_1 \cdot s_1}{\lambda\alpha_2 \cdot s_2} - \frac{\lambda\alpha_3 \cdot s_3 \cdot T_0^{s_3-s_1}}{\lambda\alpha_2 \cdot s_2} \quad (31)$$

Thus, the solution for T_0 in terms of the original parameters is:

$$T_0 = \left[-\frac{\alpha_1 \cdot s_1}{\lambda\alpha_2 \cdot s_2} \left(1 + \frac{\alpha_3 \cdot s_3}{\alpha_2 \cdot s_2} T_0^{s_3-s_2} \right)^{-1} \right]^{\frac{1}{s_2-s_1}} \quad (32)$$

C Justification of Tolerance Value

C.1 How was this determined?

Tolerance ϵ in Equation 1 depends on the importance of maintaining general abilities for CPT goals (Definition 1). We set $\epsilon = 0.05$ based on empirical results by observation. However, **the value of ϵ does not affect the conclusions and analysis** presented in this paper. In practical applications, its setting is related to the researcher's considerations of relevant factors (application scenarios, resource situation, etc.) for CPT.

As shown in Figure 4 and Figure 7, $\Delta_{\text{General loss}}$ typically peaks at values much smaller than 0.05. This is because these figures depict relatively small mixture ratios ($\mathcal{R} \leq \frac{1}{2}$), where general losses initially increase before decreasing. As the mixture ratio grows, $\Delta_{\text{General Loss}}$ continues to rise and eventually exceeds 0.05 ($\mathcal{R} \rightarrow 1$). This trend can be initially observed in Figure 1 and Figure 8.

C.2 How does this value reflect the constraint in practice?

As detailed in Definition 2, the tolerance value ϵ is used to determine a range of mixture ratios \mathbb{A} that do not lead to excessive increases in general losses (i.e., unaffordable losses in general capabilities). **In practice, we use the tolerance to identify the upper bound of feasible mixture ratios.** For example, an excessive mixture ratio may cause the general loss to exceed the tolerance threshold. Therefore, even if the general loss under this ratio reaches a plateau or decreases, it is still considered infeasible.

D Table

To illustrate the accuracy of our fitting, we provide the relative error for the fitted curves in Table 2, along with the MSE and R^2 values for the power-law fitting of Δ General (Δ Domain) loss as a function of training tokens T in Table 3. For better reproducibility, the fitted scaling law coefficients are presented in Table 4 and Table 5, which correspond to § 5.3. In summary, we found that the power function accurately fits the loss with respect to model size, data mixture ratio, and token volume, using the Scipy library to estimate the function’s coefficients.

Ratio	460M	940M	1.6B	3.1B
100%	1.4628	1.3723	1.3242	1.2585
75%	1.4844	1.3910	1.3416	1.2750
50%	1.5122	1.4155	1.3643	1.2965
33%	1.5387	1.4385	1.3854	1.3170
25%-gt	1.5561	1.4538	1.3994	1.3305
25%-pred	1.5566	1.4546	1.3999	1.3303
Difference	0.03%	0.05%	0.03%	0.02%

Table 2: Domain Proportion and Predicted/Actual Value Relative Error

Metric Ratio	General				Domain				
	460M	940M	1.6B	3.1B	460M	940M	1.6B	3.1B	
MSE	100%	1.9394e-10	2.5695e-10	9.8058e-10	2.2880e-11	9.7830e-08	7.6174e-08	6.4577e-08	4.4057e-08
	75%	5.2270e-11	7.7104e-15	3.4402e-12	1.5432e-11	1.2283e-07	7.6940e-08	7.1749e-08	4.4160e-08
	50%	1.5340e-10	4.4162e-11	1.5992e-09	1.6405e-10	1.2539e-07	7.0535e-08	5.1893e-08	3.8559e-08
	33.3%	5.2538e-11	1.1070e-10	5.5883e-11	5.4041e-11	1.1904e-07	6.9371e-08	5.8162e-08	4.4630e-08
	25%	7.3045e-11	4.7677e-11	8.7140e-11	1.6598e-14	1.0966e-07	7.0327e-08	4.7272e-08	4.6702e-08
	12.5%	6.9011e-11	8.9891e-11	7.1858e-11	9.2656e-11	8.1609e-08	7.2597e-08	5.1854e-08	4.4091e-08
	R^2	100%	0.9999	0.9999	0.9998	0.9989	0.9957	0.9969	0.9969
75%		0.9993	0.9999	0.9990	0.9963	0.9954	0.9966	0.9966	0.9975
50%		0.9973	0.9966	0.9946	0.9593	0.9951	0.9963	0.9965	0.9971
33.3%		0.9928	0.9877	0.9818	0.9251	0.9954	0.9959	0.9965	0.9967
25%		0.9872	0.9763	0.9659	0.8741	0.9956	0.9959	0.9966	0.9966
12.5%		0.9590	0.9438	0.9520	0.8972	0.9974	0.9962	0.9963	0.9965

Table 3: The MSE and R^2 of the fitting power-law of Δ General (Δ Domain) loss by training tokens T

E Figure

To comprehensively illustrate the patterns observed in our experiments and our findings, we present the evolution of loss across different mixture ratios and model sizes throughout training in Figure 8. Additionally, Figure 9 shows the extrapolation of T using a power-law fit, highlighting the variations in the rise-then-fall trend of general loss under different mixture ratios and model sizes. Finally, the changes and predictions of general loss and domain loss with respect to T under different mixture ratios are illustrated in Figure 10. This effectively explains why we use different forms of power laws to predict T in § 5.2.

Model Size	Ratio	General					Domain		
		α_1	s_1	α_2	s_2	β_1	α_3	s_3	β_2
460M	100%	-0.01502	0.17543	0.02116	0.46219	0.00472	-2.43854	0.02229	2.24461
	75%	-0.14742	0.64329	0.15135	0.63990	0.00144	257.77904	-0.00022	-257.95781
	50%	0.12446	0.57575	-0.12123	0.57941	0.00050	227.06960	-0.00023	-227.23919
	33.3%	0.11761	0.53594	-0.11471	0.53971	0.00002	97.25206	-0.00050	-97.40981
	25%	0.14030	0.51526	-0.13758	0.51836	-0.00018	24.62425	-0.00190	-24.77263
	12.5%	0.13055	0.48615	-0.12803	0.48955	-0.00055	0.71989	-0.08343	-0.81231
940M	100%	0.00987	0.51496	-0.00521	0.00000	0.00423	262.61092	-0.00021	-262.90741
	75%	0.00653	0.30806	-0.00500	0.00000	0.00232	259.14017	-0.00020	-259.43163
	50%	0.09454	0.57282	-0.09209	0.57654	0.00101	258.06226	-0.00019	-258.34505
	33.3%	0.10418	0.52619	-0.10186	0.52970	0.00063	248.51191	-0.00018	-248.78323
	25%	0.11006	0.51700	-0.10785	0.52040	0.00046	222.52376	-0.00020	-222.78786
	12.5%	0.12685	0.48822	-0.12468	0.49141	0.00013	129.70296	-0.00031	-129.94852
1.6B	100%	0.00752	0.50645	-0.00385	0.00000	0.00384	-0.39825	0.09162	0.20416
	75%	0.06381	0.63024	-0.06167	0.63444	0.00161	210.68118	-0.00023	-210.84391
	50%	0.07899	0.57219	-0.07702	0.57587	0.00084	258.78683	-0.00017	-258.94316
	33.3%	0.08952	0.54505	-0.08764	0.54858	0.00050	133.08715	-0.00032	-133.23264
	25%	0.08747	0.53775	-0.08564	0.54152	0.00034	4.92547	-0.00864	-5.06034
	12.5%	0.10378	0.51241	-0.10198	0.51585	0.00007	210.06851	-0.00018	-210.18657
3.1B	100%	0.00978	0.38822	0.00000	3.42674	0.01398	-0.30116	0.10974	-0.03868
	75%	0.04886	0.56155	-0.04660	0.56711	0.01184	265.17268	-0.00018	-265.47797
	50%	0.06324	0.52050	-0.06100	0.52592	0.01093	156.20051	-0.00027	-156.50271
	33.3%	0.08406	0.51263	-0.08187	0.51724	0.01056	128.57034	-0.00031	-128.86546
	25%	0.08084	0.51463	-0.07866	0.51973	0.01034	133.03230	-0.00028	-133.32244
	12.5%	0.09549	0.49146	-0.09320	0.49629	0.01001	7.55302	-0.00463	-7.82759

Table 4: Fitting power-law coefficients for different model sizes and the mixture ratios of Δ General and Δ Domain losses as a function of training tokens T

Model Size	α_4	s_4	β_3
460M	0.22524761	0.26944345	-0.48139982
940M	0.7520627	0.13720245	-1.06581937
1.6B	-2.36384831	-0.15125569	1.59223649
3.1B	-2.5368197	-0.42071423	0.84375368

Table 5: Fitted CPT scaling law coefficients for different model sizes in *Finance*.

Domain-General Loss Curve (Scale cross-section and Ratio cross-section)

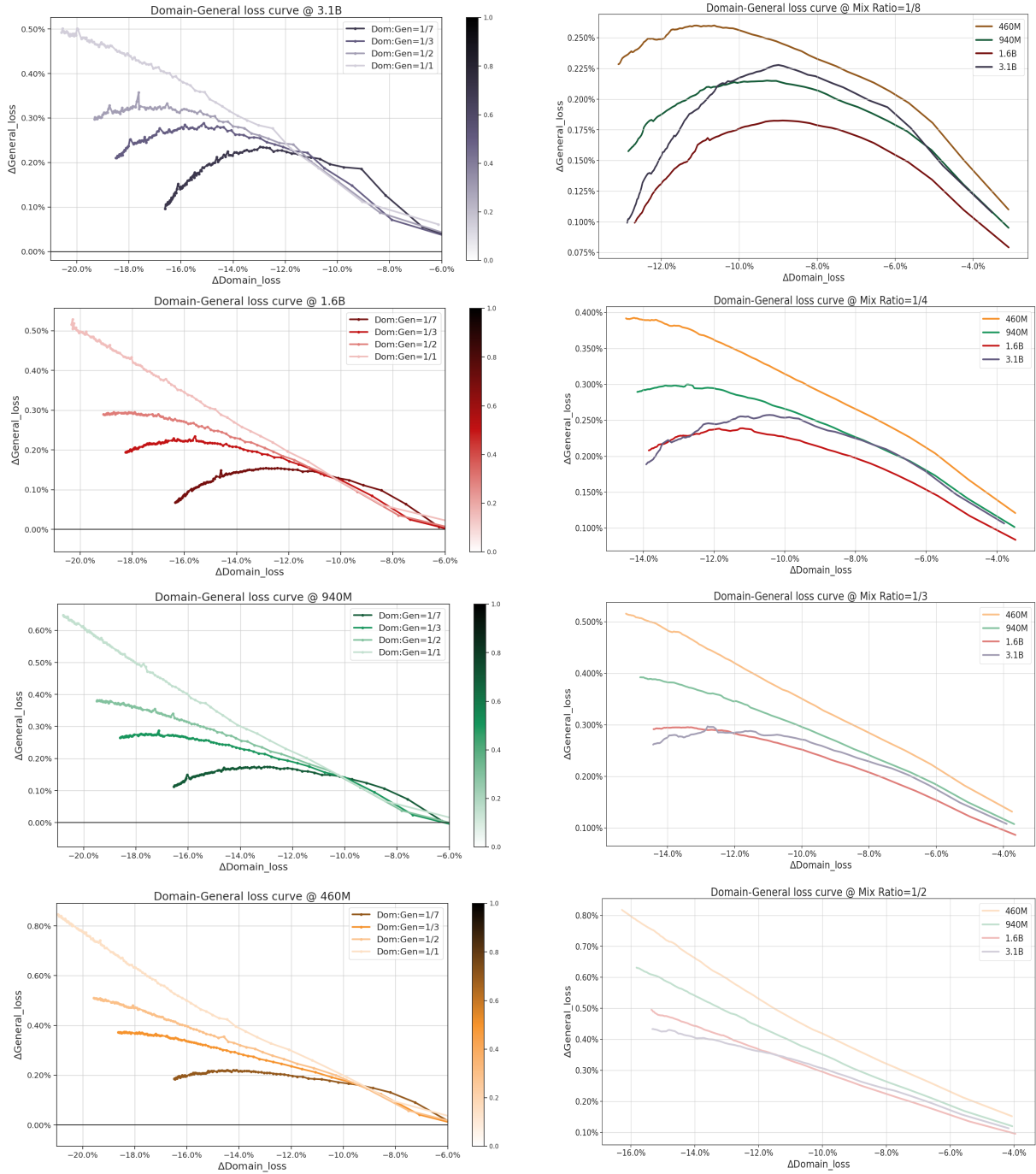


Figure 8: Each cluster represents a different mixing ratio, which is 1/8, 1/4, 1/3, 1/2. Pay attention to the third set of lines, that is, clusters with a proportion of 1/3. The cross-section of this set of lines is shown on the right.

Extrapolation of T with power law

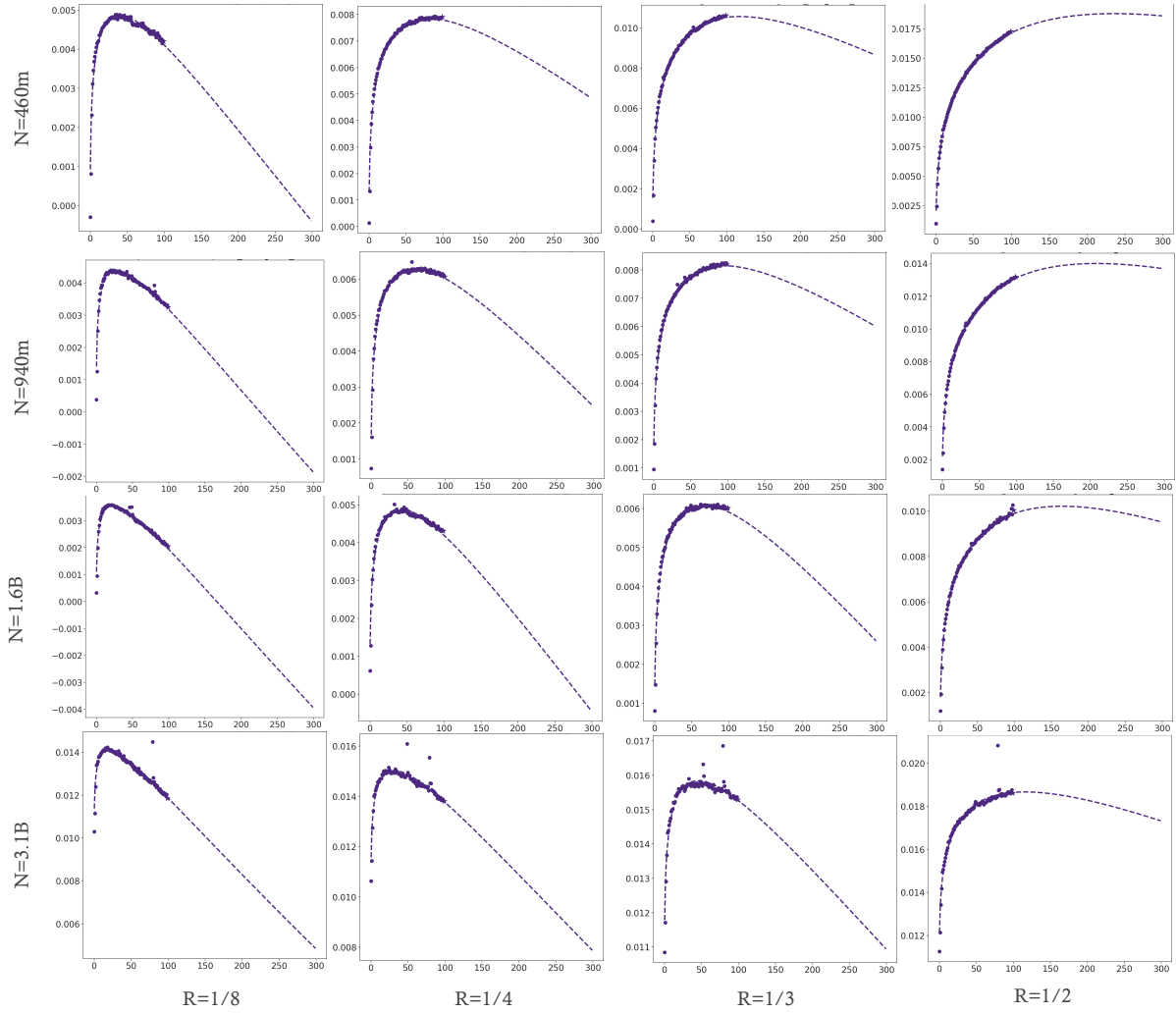


Figure 9: Power laws of training token volume for different model sizes in *Finance*. Compared with the extrapolation of the training volume of the model of the same size to continue training in the *Academic papers* field in Figure 7, it can be seen that under the same proportion, the amount of training volume of CPT of Academic Papers is larger where the inflection point appears.

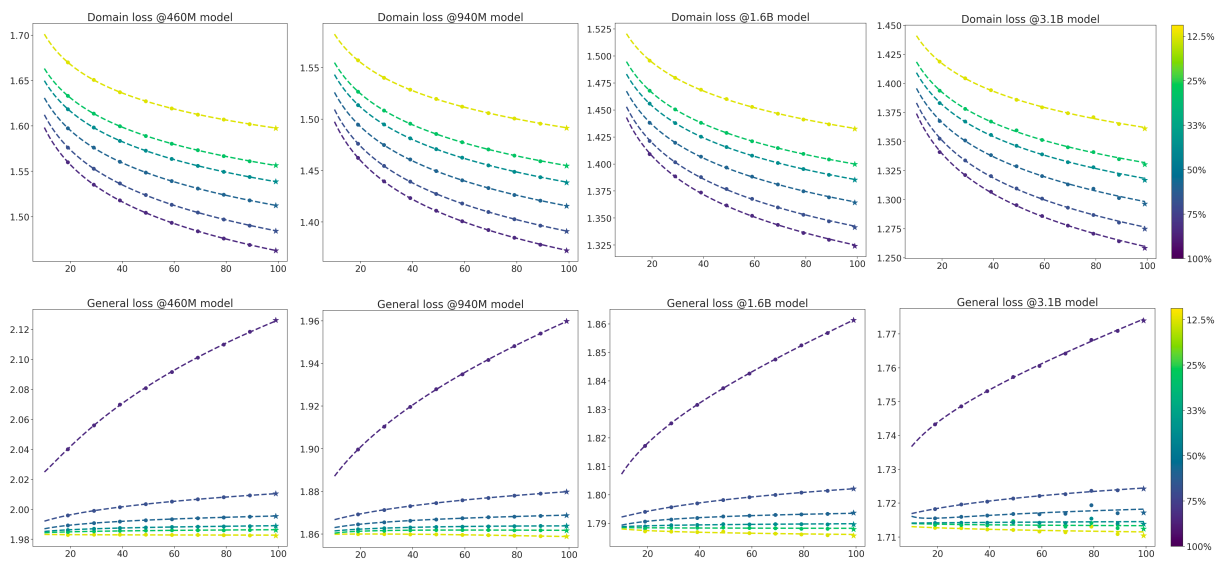


Figure 10: The temperature bar represents the mixture ratio R , which takes six values ranging from $1/8$ to 1 . Different subgraphs are fitting curves that change with the increase of T in the training process for different M_N domain loss and general loss. Overall, the domain loss keeps decreasing during the training process while the general loss keeps increasing. It is worth noting that although the general loss is increasing, the magnitude of its increase is actually very small, especially when the mixture ratio is not very big ($R = \{1/8, 1/4, 1/3, 1/2, 3/4\}$), with a total increase of less than 0.02 . The solid circles (\bullet) represent real losses, and the stars (\star) represents the predicted losses. We can see that whether it is general loss or domain loss, the predicted values fall on the fitted curves accurately.